Main Manuscript for

Cellular and Molecular Basis of Odorant Reception in the Biting Midge *Forcipomyia taiwana*

Yinxue Shan[1†], Dan Gou[1,3†], Guanzhen Fan[1], Stephen T. Ferguson[1], Lianhai Yv[3], Xiaohui Hou[3*], Feng Liu[1,2*]

1 Institute of Infectious Diseases, Shenzhen Bay Laboratory, Shenzhen, China.
2 Guangdong Provincial Key Laboratory of Infection Immunity and Inflammation, Shenzhen, China.
3 Department of Cell Biology, Zunyi Medical University, Zunyi, China.

* Corresponding author

Feng Liu, Ph.D.
Infectious Diseases Research Institute, Shenzhen Bay Laboratory; Shenzhen, Guangdong 518132, China; Email: liufeng@szbl.ac.cn; Phone: +86-0755-86724700.

Xiaohui Hou, Ph.D.

Department of Cell Biology, Zunyi Medical University; Zunyi, Guizhou 563000, China; Email: houxh1@zmu.edu.cn; Phone: +86-0851-28205801.

† These authors contributed equally to this work.

Author Contributions
Conceived and designed the study: F.L., X.H. Performed the experiments: Y.S., D.G., G.F. Prepared the materials: Y.S., D.G., L.Y. Wrote and edited the paper: Y.S., F.L., X.H., S.T.F.

Competing Interest Statement: The authors declare no competing interests.

Keywords: biting midge, olfactory sensillum, olfactory sensory neuron, olfactory receptor, behavioral response.

This PDF file includes:

Main Text
Figures 1 to 7

Abstract

Biting midges are medically significant pests whose bites trigger dermatitis and systemic allergic responses while transmitting diverse pathogens, thereby posing a severe threat to human health. How these and other blood-feeding insects parse complex odor environments to locate hosts while avoiding unfavorable cues is a fundamental question in sensory biology. However, the olfactory mechanisms underlying odorant detection in midges remain poorly understood. Here, we elucidate the neural and molecular mechanisms underlying odor-guided behavior in *Forcipomyia taiwana*, the predominant biting midge in China and Southeast Asia, using an integrated, multi-scale approach. The antennae contain diverse olfactory sensilla and a broad chemoreceptor repertoire that respond to host- and plant-derived volatiles. In contrast, spherical sensilla within the maxillary palp form a dual-channel olfactory pathway that segregates two ecologically salient classes of chemical information: one sensory neuron is strongly activated by host-associated CO_2 and the other is preferentially tuned to plant-derived terpenoids. Tissue-resolved transcriptomics, receptor localization, and heterologous functional analysis identify the palp-enriched receptor FtaiOr1 as a strong molecular determinant of this terpenoid-sensitive pathway while FtaiOr27 and FtaiOr60 localize to the antennae and detect additional odor classes. These peripheral sensory responses correspond to opposing behavioral outcomes: terpenoids, including camphor, eucalyptol, and (+)-fenchone, strongly repel *F. taiwana*, whereas human-associated volatiles such as butanal and butanoic acid promote attraction. Together, these findings link receptor identity, neuronal coding, and behavior in an understudied hematophagous insect, revealing a mechanistic framework for understanding odor-guided behavior in biting midges and suggests broader principles by which blood-feeding Diptera partition ecologically opposing olfactory information.

Significance Statement

Pathogen-carrying biting midges constitute an emerging global public health threat, as exemplified by recent outbreaks of Oropouche virus across the Americas and Europe. Commonly used insecticides trigger resistance and ecological damage, creating an urgent demand for sustainable intervention tactics. Here, we systematically decipher the cellular and molecular mechanisms mediating detection of chemical cues and their role in odor-guided behavior in *F. taiwana*. Our findings advance the fundamental olfactory biology of biting midges and provide a clear path towards the development of sustainable, eco-friendly, odor-targeted vector control technologies, thereby reducing the risk of midge bites and associated disease transmission.

Main Text

Introduction

Biting midges (Diptera: Ceratopogonidae) are hematophagous insects of substantial ecological and medical importance. Females of several midge species serve as vectors for diverse pathogens affecting humans, livestock, and wildlife, including Oropouche virus (OROV), Bluetongue virus (BTV), and *Leucocytozoon caulleryi* (1, 2). Recent outbreaks of OROV in South America highlight the growing public health relevance of these vectors (3-5). Moreover, recent environmental changes, including urbanization, deforestation, and climate change, have contributed to shifts in midge distribution and seasonal activity, intensifying the threats posed by midge-borne diseases (6, 7). Despite their capacity to transmit a wide range of pathogens, biting midges remain understudied compared to major mosquito vectors, and fundamental aspects of their biology, particularly at the molecular and cellular level, remain poorly understood. Current midge control strategies continue to rely primarily on broad-spectrum chemical pesticides, approaches limited by the evolution of resistance and undesirable chemical effects (8-10). Developing more selective and sustainable strategies will therefore require a deeper understanding of the sensory mechanisms that govern midge behavior.

Biting midges rely heavily on their olfactory system to locate vertebrate hosts, navigate complex environments, identify plant-derived resources such as nectar, and coordinate reproductive behaviors (11-13). Odor detection begins in specialized sensilla distributed across the peripheral chemosensory appendages, principally the antenna and maxillary palps, where olfactory sensory neurons (OSNs) express distinct repertoires of odorant receptors (ORs), ionotropic receptors (IRs), and gustatory receptors (GRs) (14, 15). In mosquitoes and other well-studied Diptera, these appendages exhibit substantial functional specialization. The antennae contain diverse populations of OSNs that detect broad classes of environmental and host-associated volatiles, whereas the maxillary palps contain more restricted sensory circuits specialized to detect ecologically important cues, including CO_2 (16, 17). The organization and function of these peripheral olfactory pathways have been investigated extensively in mosquitoes and *Drosophila*, providing a mechanistic framework linking receptor expression, neuronal activity, and odor-guided behavior (18-20). By comparison, our understanding of the olfactory coding in biting midges remains limited. Previous studies have described their olfactory sensilla and physiological responses to selected odorants (21-23), and recent genomic work has revealed substantial chemosensory receptor repertoires in biting midge species, including *Forcipomyia taiwana* (24). However, how these receptors are distributed across olfactory organs and sensory neurons, how individual receptor and sensilla populations encode ecologically relevant odors, and how this peripheral sensory organization ultimately related to behavior remain largely unknown.

Forcipomyia (*Lasiohelea*) *taiwana* is a strongly anthropophilic biting midge widely distributed across southern China and Southeast Asia including Malaysia, Thailand, and Myanmar (25, 26). Its bites can cause intense itching, inflammation, and severe allergic reactions (27-30), and Japanese encephalitis virus (JEV) has previously been isolated from this species, raising additional

questions regarding its potential medical relevance (31, 32). Recent work has further shown that human-associated volatiles influence host preference in *F. taiwana*, underscoring the importance of olfactory cues in its interaction with humans (13). Yet the peripheral sensory mechanisms through which *F. taiwana* detects and discriminates host-derived and environmental odorants remains poorly understood. In particular, it is unknown how olfactory function is partitioned between the antennae and maxillary palps, which chemosensory recpetors underlie the tuning of specific sensory neurons, and how physiologically active odorants translate into attraction or avoidance at the behavioral level.

Here, we address these questions through an integrated, multi-scale analysis of the *F. taiwana* olfactory system spanning sensory morphology, neurophysiology, receptor expression and function, and odor-guided behavioral bioassays. We first characterize the morphological and functional diversity of olfactory sensilla on antennae and maxillary palps using scanning electron microscopy (SEM), electroantennography (EAG), and single-sensillum recordings (SSR). We then define the chemosensory repertoires of these two appendages through tissue-resolved transcriptomics, functionally characterize selected highly expressed ORs using the *Drosophila* empty-neuron system, and localize these receptors to peripheral sensory neurons by fluorescence in situ hybridization (FISH). Finally, we connect sensory inputs to behavioral outputs by testing physiologically active host-derived volatiles and plant-derived terpenoids for their attractive or repellent effects. Together, these studies link chemosensory receptor function to neuronal coding and organismal behavior, providing a mechanistic foundation for understanding olfaction in biting midges and identifying odor cues that may lead to the development of novel, eco-friendly control strategies and the reduction of midge-borne diseases.

Results

Diverse, morphologically distinct olfactory sensillum on the antennae and maxillary palp of *F. taiwana*

In order to better understand the organization of the peripheral olfactory system in *F. taiwana*, we first examined the macrostructure of the sensilla found on the antennae and maxillary palp using scanning electron microscopy (SEM) (Fig. 1). Similar to other *Culicoides* (21), the antennae of female *F. taiwana* exhibit a conserved fundamental structure: a basal segment, the scape, the pedicel, and the flagellum composed of 13 flagellomeres (labelled F1 - F13) (*SI Appendix*, Fig. S1 and Fig. 1*B*). The proximal flagellomeres (F1 - F8) are short (Fig. 1*D*), while the distal flagellomeres (F9 - F13) are elongated (Fig. 1*C*). Notably, the types of sensilla on the short and elongated flagellomeres were markedly different. The elongated flagellomeres contain primarily two types of olfactory sensilla: long sharp trichoid sensilla (LST) and grooved peg sensilla I (GP I) (Fig. 1 *E* and *F*). The short flagellomeres primarily contained four types of olfactory sensilla: grooved peg sensilla II (GP II), short sharp trichoid sensilla (SST), long blunt trichoid sensilla (LBT), and short blunt trichoid sensilla (SBT) (Fig. 1 *G-J*). The maxillary palp of *F. taiwana* had five segments, with the third segment bearing sensory pits (Fig. 1 *K-M*).

Within this sensory pit, spherical sensilla were distributed amongst bristle-like setae (Fig. 1*N*).

Electrophysiological responses of *F. taiwana* antennae to semiochemicals

To elucidate the antennal responses of biting midges to ecologically relevant compounds, we first recorded antennal EAG responses of adult female midges to a panel of 56 plant and host-derived volatiles spanning multiple chemical categories, including terpenoids, ketones, aromatics, heterocyclics, alcohols, esters, aldehydes and carboxylic acids (Figure 2). Among this panel of odorants, the strongest EAG responses were elicited by attractive human-derived volatiles, including butanoic acid, butanal, propanal, and sulcatone (also referred to as 6-methyl-5-hepten-2-one) (33) in addition to plant-derived volatiles including linalool, (+)-fenchone, and geranyl acetate (34, 35), suggesting these compounds may encode odor valence and mediate important midge behaviors such as host-seeking and avoidance.

Functional characterization of olfactory sensilla on the antennae and maxillary palps of *F. taiwana*

To functionally characterize the olfactory sensilla of different morphological types in the midge antennae and maxillary palps, we performed SSR to examine their neuronal responses to a panel of 34 compounds of different chemical groups, including terpenoids, ketones, aromatics, heterocyclics, alcohols, esters, aldehydes and carboxylic acids. From the short, proximal antennal flagellomeres (F1-F8), we recorded responses from four sensillum types, LBT, SBT, SST and GPII (Fig. 1G-J, Fig. 3*A*). Hierarchical cluster analysis based on these responses indicated that the LBT sensilla could be divided into two classes, which we designated LBT1 and LBT2. While both LBT classes showed similarly strong responses to certain compounds such as acetophenone, 1-octen-3-ol and (+)-fenchone, LBT2 exhibited broader and higher magnitude responses across a spectrum of odorants, displaying stronger excitatory responses to certain terpenoids, ketones, aromatics, heterocyclics, and alcohols while at the same time displaying stronger inhibitory responses to certain aldehydes and acids. Additionally, LBT1 showed weak or inhibitory responses to some volatiles like 2-methylphenol, 1-butanol, 1-pentanol, and methyl acetate. Dose-response analyses for acetophenone and 1-octen-3-ol further demonstrated that the responses of LBT sensilla to both compounds increased progressively with rising concentration (Fig. 3*B*).

Hierarchical cluster analysis revealed that SBT sensilla fell into two classes, which were designated as SBT1 and SBT2 (Fig. 3*A*). SBT1 exhibited strong excitatory responses to various aldehydes, aromatic, carboxylic acids, and alcohols, with the strongest response elicited by human odorant heptanal, which evoked a mean response of 114.00 ± 15.76 spikes/s (Fig. 3*A*). In contrast, SBT2 displayed a much narrower excitatory response spectrum, showing strong excitatory responses only to several aldehydes such as butanal, pentanal, 1-octen-3-ol, and hexanal (Fig. 3*A*). Dose-response analyses for heptanal, butanal, and butanoic acid demonstrated that the responses of SBT sensilla to all three compounds increased with increasing concentration (Fig. 3 *C*).

For SST sensilla, significant excitatory responses were only observed following stimulation with a few compounds, including acetophenone, octanal, heptanal, nonanal, and butanoic acid, with maximum neuronal responses of 112, 94, 118, 106, and 80 spikes/s, respectively (Fig. 3*A*). GPII sensilla exhibited no significant excitatory responses to any of the tested odorants (Fig. 3*A*). Both SST and GPII sensilla displayed inhibitory responses to multiple compounds, such as limonene and 2-hexaone.

In addition, we examined the functional categories of two morphologically different sensillum types, LST and GPI, on the antennal elongated flagellomeres (F9-F13) to the same panel of compounds (Fig. 3*A*). Hierarchical cluster analysis revealed that GPI sensilla comprised two classes, designated GPI1 and GPI2. GPI1 exhibited strong excitatory responses only to butanoic acid, pentanoic acid, and pentanal, with mean responses of 52.67 ± 18.77, 87.33 ± 10.73, and 58.67 ± 11.39 spikes/s, respectively. In the response spectrum of GPI2, strong excitatory responses were observed only upon stimulation with 4,5-dimethylthiazole and 2-methylphenol, with neuronal responses of 114 and 90 spikes/s, respectively. Similar to GPII sensilla from the short flagellomeres, LST displayed no strong excitatory responses to any of the tested odorants (Fig. 3*A*). We speculate that these two sensillum types may exhibit stronger excitatory responses to compounds outside the panel tested in the present study. Furthermore, multiple compounds elicited varying magnitudes of inhibitory responses in both LST and GP1.

Previous studies have indicated that mosquito maxillary palps are pivotal for the detection of carbon dioxide (CO_2), host volatile cues (1-octen-3-ol), and/or plant volatiles (16, 35). To explore the functional roles of maxillary palps in midges, we first performed SSR on spherical sensilla within the sensory pits of maxillary palps. This sensillum contains two olfactory receptor neurons (ORNs), designated A neuron with a large amplitude and B neuron with a small amplitude (Fig. 3*D*). Interestingly, the larger A neuron of midge palps exhibits particularly strong responses to carbon dioxide (Fig. 3 *E* and *F*), a functional characteristic analogous to that of the A neuron within the capitate-peg sensilla on mosquito maxillary palps (27-29). In contrast, two additional compounds, pyridine and 2-methyl-2-thiazoline, which were previously reported to activate the CO_2-sensitive neurons in mosquito (36), evoked no responses in the A neurons of biting midge (Fig. 3*F*). Furthermore, we observed that the B neuron showed robust excitatory responses to terpenoids including (+)/(-)-fenchone, camphor, and eucalyptol, whereas no responses to 1-octen-3-ol (Fig. 3 *G, H* and *SI Appendix,* Fig. S2).

Expression profiling of chemosensory receptor genes in the head of *F. taiwana*

To investigate the molecular mechanisms underlying olfactory perception in midges, we first performed transcriptome sequencing on the full heads of adult female midges. Here, we renamed the annotated *F. taiwana* ORs (*FtaiOrs*), IRs (*FtaiIrs*), GRs (*FtaiGrs*) according to their phylogenetic relationship (*SI Appendix*, Table S1)(24). The results showed that 58 OR genes were substantially expressed in the head (TPM > 1) (Fig. 4*A*). As expected, *FtaiOrco* was the most highly expressed gene among all ORs, which is consistent with its essential role as a universal co-receptor for OR-mediated odor detection (37). Additionally, we found that 26

GR genes and 35 IR genes were also substantially expressed in the midge head (*SI Appendix*, Fig. S3). Here, we focus our analyses on OR, IR, and GR transcripts with TPM > 1, however, the complete expression data are provided in the SI Appendix (Table S2).

To more precisely determine the transcriptomic abundance of chemosensory receptor genes in the olfactory appendages, we performed ultra-low input transcriptomic RNA sequencing with tissue-specific antennae or maxillary palp samples from adult female midges (Fig. 4*B*). We first conducted expression profiling of 58 ORs in the antennae and maxillary palps. The results revealed that the co-receptor *Orco* exhibited high expression in both chemosensory tissues (Fig. 4 *C* and *D*). A total of 13 OR genes were enriched in the antennae with a TPM higher than 100. In contrast, overall expression levels were relatively low in maxillary palps, with only two OR genes enriched in this tissue (*FtaiOr1*, *FtaiOr76*). Notably, *FtaiOr1* exhibits tissue-specific expression in the maxillary palps (Fig. 4*D*).

In addition, among the 35 IRs with substantial expression in the head, 14 IR genes were highly expressed in the antennae (TPM > 10), whereas only four were highly enriched in the maxillary palps (Fig. 4 *C* and *D*). Among these, the ionotropic receptor co-receptor *IR25a* (*FtaiIr25a*) exhibited the highest transcriptomic abundance in both tissues. Notably, prior phylogenetic analyses of IRs annotated from the *F. taiwana* genome failed to recover IR8a and IR76b orthologs with that of *D. melanogaster* and *Ae. Aegypti* (24). This apparent failure to detect orthologs may stem from the limited contiguity of the genome assembly, which impedes the prediction of full-length gene models.

Of the 26 gustatory receptor (GR) genes expressed in the head, eight exhibited high expression in maxillary palps (Fig. 4*D*). Among them, *FtaiGr13*, *FtaiGr14* and *FtaiGr15* showed prominent maxillary palp-specific expression, and phylogenetic analyses revealed that that these three gustatory receptors are homologous to the canonical CO_2-sensing receptor triad AaegGr1, AaegGr2 and AaegGr3 from *Aedes aegypti*, with amino acid sequence identities of 69%, 75% and 60%, respectively (*SI Appendix*, Fig. S4) (24). Consistent with these findings, single sensillum recordings from spherical sensilla housed in the maxillary palp olfactory pits revealed robust neuronal activation by CO_2 (Fig. 3 *E* and *F*). This suggests that *FtaiGr13/14/15* are likely expressed in these spherical sensilla, where they assemble into a conserved CO_2 receptor complex to mediate CO_2 detection during host-seeking behavior.

Functional deorphanization of *FtaiORs* with the *Drosophila* “empty” neuron system

To further unravel the molecular basis of odorant recognition in the biting midge, we attempt to decipher the response profiles of midge ORs through the *Drosophila* “empty” neuron system. We initially selected the top 20 *FtaiOr* genes with the highest transcription abundance in the heads of *F. taiwana* for functional characterization (Fig. 4*A*). When we performed SSRs on ab3A neuron (housed in ab3 sensilla) expressing each of these 20 OR genes, we found that 14 of them (*FtaiOr5*, *FtaiOr11*, *FtaiOr14*, *FtaiOr16*, *FtaiOr19*, *FtaiOr26*, *FtaiOr36*, *FtaiOr58*, *FtaiOr61*, *FtaiOr62*, *FtaiOr70, FtaiOr75*, *FtaiOr76*, and *FtaiOr79*) failed to be properly expressed in the ab3A neuron with either no spike or abnormal burst spikes (*SI Appendix*, Fig.

S4). Only ab3A neuron expressing *FtaiOr1*, *FtaiOr12*, *FtaiOr20*, *FtaiOr27*, *FtaiOr60*, and *FtaiOr124* exhibited stable, consistent spikes (*SI Appendix*, Fig. S5). We examined the neuronal responses of target sensilla expressing each of these six *FtaiOr* genes to a broad panel of odorants (180 compounds) covering both human- and plant-drived volatiles (*SI Appendix*, Table S3). The results showed that *FtaiOr12*, *FtaiOr20*, and *FtaiOr124* did not respond to any of the tested compounds (response <10 spikes/s), whereas *FtaiOr1*, *FtaiOr27*, and *FtaiOr60* were activated by a subset of the odorants (Fig. 5 and *SI Appendix*, Fig. S6).

Specifically, we found that FtaiOr1 showed a highly specific yet broadly tuned excitatory response to the tested compounds, particularly the terpenoids, while also showing significant inhibition by some others (Fig. 5*A*). Fourteen monoterpenoids triggered exceptionally strong activation (mean responses > 100 spikes/s, Fig. 5 *D and G*). Dose-response assays revealed that the responses of FtaiOr1 to eight of the most potent compounds ((*S*)-cis-verbenol, α-terpineol, α-(-)-thujone, terpinolene, eucalyptol, camphor, (+)-fenchone, (-)-fenchone) are concentration-dependent (Fig. 5*J*). Interestingly, (+)-fenchone and (-)-fenchone served as the most potent ligands eliciting nearly identical response, indicating no chiral differentiation by the FtaiOr1. Additionally, strong excitatory responses were also elicited by other terpenoids and aromatic compounds, including (+)-neomenthol, β-myrcene, 2-ethyltoluene, 3-carene, 1S-(+)-3-carene and naphthalene (mean response > 50 spikes/s; <100 spikes/s, Fig. 5*D*). Overall, FtaiOr1 is a broadly tuned olfactory receptor with a strong response bias towards plant-derived terpenoids (*K*=5.88).

FtaiOr27 also displayed distinct sensitivity and selectivity to certain terpenoids within the large tested panel (Fig. 5*B*). Moderate to strong excitatory responses (mean response 44.4 to 65.6 spikes/s) were elicited only by a small subset of monoterpenoids, including (+)-fenchone, camphor, α-thujone, eucalyptol, (+)-fenchone, and (*S*)-cis-verbenol (Fig. 5 *E and H*), with response increasing in a dose-dependent manner (Fig. 5*K*). The vast majority of remaining compounds elicited weak activation or inhibition or no response at all. These results indicate that FtaiOr27 is a narrowly tuned odorant receptor (*K*=19.28) specifically tuned to a few terpenoid compounds.

In addition, FtaiOr60 displayed a relatively broad response profile (Fig. 5*C*). It can be effectively activated by various ketones, esters and a few terpenoids (Fig. 5 *F and I*). Among them, 2-heptanone, isoamyl acetate, hexyl acetate, 2-nonanone, E-2-hexenyl acetate and 2-decanone elicited robust excitatory responses (mean response >100 spikes/s), while 19 compounds including cyclohexanone, ethyl octanoate, phenethyl acetate, and (+)-fenchone elicited strong activation (mean response > 50; <100 spikes/s). Dose-response assays revealed that the response of FtaiOr60 to hexyl acetate, (*E*)-2-hexenyl acetate, 2-decanone, 2-nonanone and isoamyl acetate increased significantly in a concentration-dependent manner (Fig. 5*L*). Moreover, FtaiOr60 displayed prominent inhibitory responses to multiple terpenoids and aromatic compounds, with naphthalene, (+)-carvone, and β-caryophyllene exerting the strongest inhibitory effects. Collectively, FtaiOr60 is a broad-spectrum odorant receptor with high preference for esters and ketones (*K*=2.52), which may play a vital role in olfactory

perception during host seeking and environmental navigation.

Spatial localization of OR genes in antennae and maxillary palp

Next, we first performed whole-mount fluorescence in situ hybridization (WM-FISH) to characterize the spatial expression pattern of *FtaiOrco* in the antennae. Probes were labeled with Cy3 (red), and nuclei were counterstained with DAPI (blue). As expected, fluorescent signals showed that *FtaiOrco* was widely distributed on the antennal flagellum, with positive labeling primarily located in the somata of olfactory neurons underlying olfactory sensilla (Fig. 6 *A*-*D*).

Next, we examined the spatial organization of three functionally characterized *FtaiOrs* (*FtaiOr1*, *FtaiOr27*, *FtaiOr60*). RNA-seq profiling of antennae and maxillary palps demonstrated that *FtaiOr1* exhibits palp-specific expression, while *FtaiOr27* and *FtaiOr60* are exclusively expressed in antennae (Fig. 4 *C* and *D*). Therefore, we performed WH-FISH to identify the olfactory sensillum types expressing *FtaiOr1* in maxillary palps, as well as *FtaiOr27* and *FtaiOr60* in antennae. Our labeling results demonstrated strong *FtaiOr1* signal enrichment within the cells surrounding the sensory pit, which contained an assemblage of spherical sensilla (Fig. 6 *E*-*H*). We chose the top 20 compounds triggering maximum responses of FtaiOr1 (Fig. 5*D*) and compared their electrophysiological response profiles with spherical sensillum B neurons via Pearson correlation. A strong positive correlation was observed (r = 0.8845, $P < 0.0001$), indicating matched odor tuning between FtaiOr1 and spherical sensillum B neurons (*SI Appendix*, Fig. S8). Collectively, these findings indicate that *FtaiOr1* likely localizes to B neurons of spherical sensilla in sensory pit and is responsible for the recognition of terpenoids like fenchone. Furthermore, *FtaiOr27* showed expression in cells under long blunt trichoid sensilla on the short, proximal flagellomeres (Fig. 6 *I*-*L*). *FtaiOr60* showed strong labeling of cells underneath long sharp trichoid sensilla on the long, distal flagellomeres (Fig. 6 *M*-*P*). No distinct fluorescent hybridization signals were detected in negative control antennae and maxillary palps hybridized with sense probes targeting *FtaiOrco*, *FtaiOr1*, *FtaiOr27*, and *FtaiOr60*, confirming the specificity of the antisense probes (*SI Appendix*, Fig. S7).

Behavioral responses of *F. taiwana* to physiologically active compounds

There are numerous studies reporting that terpenoids, as major constituents of essential oils, play a pivotal role in repelling mosquitoes and other insects (38). In this study, we adopt the Standard World Health Organization (WHO) spatial repellency assays (Fig. 7*A*), to assess the behavioral responses of *F. taiwana* to six terpenoids that evoked strong neuronal responses in OSNs or Ors, including (+)-fenchone, camphor, eucalyptol, terpinolene, α-terpineol, and (S)-cis-verbenol at 0.1% and 1% dilutions. DEET was used as a positive control (39, 40), while paraffin oil and DMSO served as negative, solvent controls. At 1% dilution (Fig. 7*B*), all six tested terpenoid compounds elicited significant spatial repellency against *F. taiwana* relative to the solvent control (all $P < 0.01$), with mean repellency indices (RI) ranging from 44.17% to 88.83%. Camphor (88.83 ± 5.68%), eucalyptol (87.67 ± 4.68%), and (+)-fenchone (83.17 ±

3.13%) exhibited the strongest repellent activity, with efficacy significantly greater than that of DEET (51.83 ± 4.89%; $P < 0.0001$). By contrast, α-terpineol (71.83 ± 4.29%) and terpinolene (68.83 ± 3.83%) showed numerically higher RI than DEET, although the differences were not statistically significant. At 0.1% dilution (Fig. 7*C*), the repellent efficacy of all tested compounds against *F. taiwana* decreased. Nonetheless, camphor, eucalyptol, and (+)-fenchone still exhibited significant repellency relative to the solvent control ($P < 0.01$). Among these, camphor (43.17 ± 4.94%) and eucalyptol (42.67 ± 5.57%) remained the most potent, which were significantly higher than that of DEET (20.17 ± 3.77%; $P < 0.05$). Overall, all six tested terpenoids exhibited dose-dependent spatial repellency against *F. taiwana*, among which camphor, (+)-fenchone, and eucalyptol demonstrated the most potent midge repellency.

Given that human-derived volatiles are candidate host cues, we next examined the attraction of *F. taiwana* to the physiologically active compounds in behavioral assays (41). The attractant preferences of *F. taiwana* to four human volatile compounds (butanoic acid, butanal, propanal, and acetophenone) were assessed using a Y-tube olfactometer, with paraffin oil used as the solvent control (Fig. 7*D*). In addition, geranyl acetone, a human-derived volatile previously reported to elicit strong attraction in *F. taiwana*, was selected as the positive control (13). Our results showed that, at a concentration of 0.01%, all five tested human volatiles displayed significant attracting effects on *F. taiwana* relative to the solvent control ($P < 0.01$, Fig. 7*E*). Among these compounds, butanal and acetophenone exhibited the strongest attractiveness, with preference indices of 0.65 ± 0.13 and 0.48 ± 0.23, respectively ($P < 0.0001$). Moreover, the attraction effect of butanal was significantly higher than that of geranyl acetone ($P < 0.05$). When the compound concentration was increased to 0.1%, *F. taiwana* exhibited significant preference only for butanoic acid ($P < 0.001$, Fig. 7*F*). The reduced attractant activity of human volatiles observed at the high concentration may be explained by the biphasic dose-response property of the insect olfactory system: attraction diminishes and may even switch to repellency as compound concentration increases. This phenomenon has also been documented in previous reports on biting midges as well as other blood-feeding insects (13, 42, 43).

Discussion

Biting midges represent an ecologically and medically important group of hematophagous insects, yet the cellular and molecular organization of their olfactory systems remains poorly understood compared with that of mosquitoes. Here, we establish a multiscale framework for peripheral odor coding in *F. taiwana* by linking the structural organization of olfactory sensilla with native sensory-neuron physiology, tissue-resolved chemoreceptor expression, heterologous receptor function, receptor localization, and odor-guided behavior. Collectively, our findings reveal a pronounced functional division of labor between the two principal olfactory appendages. The antennae contain a morphologically diverse complement of sensilla and broadly sample host-associated and environmental volatiles, whereas the maxillary palps contain a more restricted sensory system dedicated to the detection of highly salient chemical

cues. Most notably, the spherical sensilla within the maxillary palp sensory pit house a CO_2-sensitive neuron together with a second neuron strongly responsive to plant-derived terpenoids. The response profile of this terpenoid-sensitive neuron closely matches that of the palp-enriched receptor FtaiOr1, and several of its strongest ligands elicit robust spatial avoidance by *F. taiwana*. These findings extend our mechanistic understanding of insect olfaction beyond the established mosquito models and suggest that distinct peripheral olfactory appendages partition chemical information according to ecological relevance.

The antennae of *F. taiwana* appear to function as broad chemical-surveillance organs. Six morphologically distinct olfactory sensilla were identified across the short proximal and elongated distal flagellomeres, and electrophysiological recordings revealed responses to compounds spanning multiple chemical classes (Figs. 1-3). Variation in the abundance and distribution of antennal sensilla has previously been reported among *Culicoides* biting midge species differing in host preferences. In the anthropophilic *F. taiwana*, we observed a greater diversity and abundance of grooved peg sensilla compared to zoophilic Culicoides midges which possess two additional antennal sensillar types, the sensilla ampullacea and sensilla coeloconica (21). Whether these interspecific variations in sensillum type and abundance contribute to the ecological specialization and the mediation of host preference among these species remains an interesting question for future comparative studies to resolve.

Consistent with the strong anthropophilic behavior of *F. taiwana*, the female antennae exhibited robust responses to several human-derived volatiles, including butanoic acid, butanal, and propanal (Fig. 2). By contrast, in zoophilic *Culicoides* species, including *C. imicola*, *C. impunctatus*, and *C. nubeculosus*, strong responses were observed to butanone, a typical odor component of livestock (22, 23). Collectively, these results indicate that differences in antennal sensilla composition and odor tuning may constitute an important neurophysiological basis for host preference. Determining whether differences in sensilla composition or receptor expression causally contribute to host specialization will ultimately require comparative analyses across midge species with distinct host preferences.

At the level of individual sensilla, the antennal responses also revealed substantial functional diversity that is not captured by morphology alone. Sensilla assigned to the same morphological class frequently differed in their odor-response profiles, indicating that visually similar sensilla may contain functionally distinct sensory-neuron populations. Compared with other sensillum types, the blunt trichoid sensilla (LBT and SBT) exhibited a very broad response spectrum, responding to a wide range of compounds, including terpenoids, ketones, aromatics, heterocyclics, aldehydes, and carboxylic acids (Fig. 3*A*). This broad receptive range differs from that described in several mosquito species, in which odor classes are more strongly partitioned among morphologically and molecularly distinct sensilla populations. In both *Anopheles gambiae* and *Ae. aegypti*, for example, blunt trichoid sensilla primarily detect a range of alcohols and terpenoids, whereas heterocyclics and aromatics are mainly detected by the morphologically distinct sharp trichoid sensilla (44-46). Moreover, we also found GPI-1 sensilla showed particular sensitivity to aldehydes and carboxylic acids. In both the fly and

mosquito, aldehydes and carboxylic acids are frequently detected by IR-expressing OSNs housed in basiconic sensillum (47, 48), suggesting that some midge grooved peg neurons may similarly employ IR-mediated detection. However, receptor expression has not yet been resolved at the level of individual grooved peg neurons in *F. taiwana*, and this hypothesis will require direct molecular localization. More generally, these results emphasize that morphological classification alone provides an incomplete description of the midge peripheral olfactory system and that neuronal identity is better understood through the integration of morphology, physiology, and receptor expression.

The organization of the maxillary palp provides a particularly striking example of such functional specialization. Here, we identified a sensory pit housing multiple spherical sensilla which contain two physiologically distinguishable neurons: a large-amplitude A neuron that responds strongly to carbon dioxide and a small-amplitude B neuron that is robustly activated by terpenoids such as (-)-fenchone, (+)-fenchone, camphor, and eucalyptol (Fig. 3*D*-*H*). CO_2-sensitive neurons have previously been described in the maxillary palps of biting midges, and specialized palpal CO_2 detection is also a prominent feature of the mosquito olfactory system (16, 49). Correspondingly, three orthologous Grs (FtaiGr13, 14, 15), are strongly encriched in the *F. taiwana* maxillary palps and show substantial sequence similarity to the canonical mosquito CO_2 receptors. Their expression pattern, sequence conservation, and the physiological activity of the palpal A neuron together identify these GRs are strong candidates for components of the midge CO_2 receptor complex.

The neighboring B neuron reveals an additional function of the biting-midge maxillary palp. Tissue-resolved transcriptomics identified *FtaiOr1* as strongly enriched in the palp, and fluorescence in situ hybridization localized *FtaiOr1* expression to cells associated with the spherical sensilla of the sensory pit (Figs. 4 and 6). When expressed heterologously in the *Drosophila* empty neuron system, FtaiOr1 responded broadly but preferentially to terpenoids, with a particularly strong activation by compounds including fenchone, camphor, eucalyptol, α-terpineol, terpinolene, and (S)-cis-verbenol (Fig. 5). Notably, the ligand-response profile of FtaiOr1 closely matched that of the native palpal B neuron (Pearson's $r = 0.8845$, $P < 0.0001$). Together, the tissue-specific expression, spatial localization, and highly correlated physiological tuning strongly support FtaiOr1 as a major molecular determinant of terpenoid sensitivity in the B neuron. Genetic disruption of *FtaiOr1* will nevertheless be required to establish its necessity for native neuronal responses and, importantly, to determine whether this receptor is causally required for terpenoid avoidance.

This palpal organization has intriguing parallels with recent findings in mosquitoes. Maxillary palps have traditionally been associated with strong CO_2 detection, although additional odor-sensitive palpal neurons have long been recognized in mosquitoes (16, 49). Recent work has further identified a specialized maxillary-palp pathway in culicine mosquitoes in which Or49-expressing neurons were found to respond strongly to bicyclic monoterpenoids, including borneol and camphor, and contribute to behavioral repellency (35). Collectively, these results reveal a striking similarity between in the peripheral sensory organization of *F. taiwana*

and mosquitoes, in which a CO_2-sensitive palpal neuron occurs alongside a distinct terpenoid-sensitive neuron. The precise evolutionary relationship between these pathways—whether FtaiOr1 and the mosquito Or49 represent homologous components of an ancestrally conserved palpal neurocircuit or whether different dipteran lineages independently recruited distinct ORs to detect similar environmentally relevant terpenoids—presents an intriguing question for future studies. Resolving this question through comparative receptor phylogenetics and functional analyses across taxa could reveal whether the juxtaposition of CO_2 and terpenoid detection represent a conserved or repeatedly evolved organizational principle in the olfactory systems of hematophagous Diptera.

The functional characterization of FtaiOr1 also begins to connect the chemoreceptor repertoire of *F. taiwana* to defined sensory circuits. Previous genome analysis revealed a substantial expansion and diversification of odorant receptors in this species (24), but the functions and cellular distributions of most of these receptors have remained unknown. Here, tissue-resolved RNA sequencing demonstrated that this receptor diversity is distributed unequally between the major olfactory appendages: the antennae express a broad repertoire of ORs, whereas relatively few are strongly enriched in the maxillary palp (Fig. 4). Functional analysis further revealed contrasting ligand spaces among the receptors examined. FtaiOr1 was broadly responsive but strongly biased towards terpenoids, FtaiOr27 showed comparatively narrow tuning to a subset of terpenoids, and FtaiOr60 responded broadly to ketones and esters while also exhibiting inhibition by several terpenoids and aromatic compounds (Fig. 5). FISH localized FtaiOr27 and FtaiOr60 to distinct antennal sensillar populations, providing an initial molecular map of odor coding across the *F. taiwana* antenna. Together, these observations begin to translate genomic receptor diversity into differences in tissue distribution, neuronal context, and chemical tuning.

At the same time, the heterologous receptor experiments reveal an important technical limitation of the present study. Only six of the 20 highly expressed FtaiOrs selected for characterization produced stable, interpretable activity in the *Drosophila* “empty” neuron system, and three of these responded to the odor panel tested. Heterologous performance can depend strongly on receptor trafficking and receptor/co-receptor compatibility targeting (48, 50-53). Moreover, the reference genome assembly, which failed to identify highly conserved IR co-receptors IR8a and IR76b, may contain fragmented or otherwise incomplete gene structure predictions (24). Alternative heterologous expression systems such as *Xenopus laevis* oocytes and HEK293 cell lines could be utilized in follow-up studies to overcome this technical bottleneck (48, 50-52). Native sensilla recordings also indicate that further sensory diversity remains unresolved. For example, FtaiOr60 was localized beneath LST sensilla, yet the limited number of LST preparations screened did not display strong excitatory responses to the odorants tested. This discrepancy may reflect heterogeneity among morphologically similar LST sensilla or incomplete sampling of rare neuronal subtypes. Resolving receptor expression at single-cell resolution will therefore be an important next step toward comprehensively mapping the midge peripheral olfactory system.

Importantly, physiological sensitivity to the compounds identified here corresponds to distinct behavioral outcomes. All six terpenoids selected on the basis of strong neuronal or receptor activity produced significant spatial repellency at the higher concentrations tested, with camphor, eucalyptol, and (+)-fenchone producing particularly strong avoidance (Fig. 7B,C). At 1%, each of these three compounds produced greater repellency than DEET, while camphor and eucalyptol also exceeded DEET at 0.1%. Conversely, several human-associated volatiles that elicited strong antennal responses produced attraction in Y-tube assays, with butanol and acetophenone among the strongest attractants at 0.01% (Fig. 7E). Previous studies have likewise demonstrated behavioral responses of *F. taiwana* and other hematophagous insects to human-associated volatiles (13, 42, 43), while plant terpenoids and essential-oil constituents are widely recognized as sources of insect-repellent (54-60). Thus, the compounds identified here provide a mechanistically informed starting point for the development of odor-based approaches to midge management. In particular, camphor, eucalyptol, and fenchone warrant further evaluation as spatial repellents, while butanal, acetophenone, butanoic acid, and related human-associated volatiles may contribute to improved attractant blends.

In summary, our study provides a cellular and molecular framework for understanding peripheral olfactory coding in an understudied lineage of hematophagous Diptera. The antennae and maxillary palps of *F. taiwana* are not simply redundant odor-detecting appendages but differ markedly in sensory architecture, receptor repertoire, and chemical tuning. The antennae broadly sample diverse host-associated and environmental odors, whereas the maxillary palp contains a compact circuit in which CO_2- and terpenoid-sensitive neurons detect two highly salient classes of chemical information. Linking the latter neuron to the palp-enriched terpenoid receptor FtaiOr1 provides the first mechanistic connections between receptor identity, native neuronal tuning, and behavior in a biting midge. Together with emerging evidence for specialized terpenoid-sensitive palpal pathways in mosquitoes (35), these findings raise broader questions about how blood-feeding Diptera have organized peripheral sensory systems to discriminate cues associated with hosts, resources and environmental hazards. More broadly, they establish *F. taiwana* as a comparative model for investigating how the evolution and diversification of peripheral chemosensory systems shape ecologically relevant behavior.

Materials and Methods

Experimental Insects. As it is difficult to propagate *F. taiwana* in a laboratory, all individuals used in this study were collected from the same field site. Species identification was performed based on COI sequences and the taxonomic characteristics described in Yu et al (26, 61). Adult midges were captured using the human bait method at Dayan Mountain Park in Guangming District, Shenzhen, Guangdong Province (22.7119° N, 113.9189° E). In brief, the experimenter allowed female biting midges to land on their lower legs, and landing midges were then captured and collected in 12 × 75 mm plastic vials and transported to the laboratory for subsequent identification and experimentation.

Scanning Electron Microscopy. The heads of adult female *F. taiwana* were dissected and immediately fixed in 4% paraformaldehyde solution for 24 h. A gradient of ethanol concentrations (30%, 50%, 70%, 80%, 90%, and 100%) was used for the dehydration process. Samples were then processed in a critical point dryer (K850, Quorum, UK). Antennae were mounted on sample stubs with conductive adhesive tape, coated with gold in a sputter coater (EM ACE600, Leica, Austria), and observed under a scanning electron microscope (GeminiSEM 360, Zeiss, Germany).

Electroantennograms. Electroantennogram (EAG) recordings were performed following a protocol described by Pelletier et al. (62) with minor modifications. Briefly, the head of an adult *F. taiwana* female was excised and mounted on an EAG platform equipped with two micromanipulators and a high-impedance AC/DC preamplifier (PRS-1, Syntech, Germany). Chlorinated silver wires in glass capillaries filled with 0.1% KCl and 0.5% polyvinylpyrrolidone were used for both reference and recording electrodes. One antenna with the tip cut was accommodated into the recording electrode. The airflow across the preparation was maintained constant at 20 ml/s to which a stimulus pulse of 2 ml/s was delivered for 500 ms. Any change in antennal deflection induced by the stimuli or control puffs was recorded for 10 s. All compounds were dissolved in DMSO or paraffin oil to make a test solution of 10-fold dilution. An aliquot (10 µl) of a tested compound was loaded onto a filter paper strip (4 × 30 mm), which was immediately inserted into a Pasteur pipette for evaporation. Solvent alone served as control. For each compound, EAG responses of 5 female midges were recorded. These recordings were analyzed using EAG software (Version 2.7, Syntech). The EAG response (ΔmV) to each test stimulus was calculated by subtracting the value of the antennal response elicited by the solvent from that stimulated by the compound. -

Single-Sensillum Recordings for Midges. Single sensillum recordings (SSR) in midges were performed in accordance with the protocols established for mosquitoes in the referenced literature (63). Female adult midges were anesthetized on ice (~30 s) and then placed into the tip of a 200 µL plastic pipette, with a small portion of the pipette tip cut off to expose the midge's head. The midge was immobilized with absorbent cotton, and the pipette tip was fixed onto a glass slide with dental wax. Two tungsten microelectrodes were electrolytically sharpened in a 10% KNO2 solution under a voltage of 2-10 V. Under a high-magnification microscope, the grounded reference electrode was inserted into the compound eye of the midge, while the recording electrode, connected to a preamplifier (Universal AC/DC 10×, Syntech, Netherlands), was inserted into the shaft of an olfactory sensillum to establish a complete circuit for extracellular recording of ORN potentials. Controlled manipulation of the recording electrode was performed using a micromanipulator (PCS-6000, Burleigh, USA). The preamplifier was connected to an analog-to-digital signal converter (IDAC-4, Syntech, Netherlands) and linked to a computer, with signal recording and visualization carried out using AutoSpike v3.9 software. Signals were recorded for 10 s, starting one second before stimulation. Action potentials were quantified offline over a 500-ms period before and after stimulation. Neuronal response strength was calculated as the total spike frequency during the 500-ms stimulus period minus

the spontaneous spike frequency during the 500-ms pre-stimulus period and expressed in units of spikes·s^{-1}.

All candidate compounds were diluted to a final concentration of 1% (v/v) using paraffin oil or DMSO. A 10 μL aliquot of each compound was applied onto a filter paper strip (4 mm × 30 mm), which was then inserted into a Pasteur pipette to create the stimulus cartridge. Samples containing only solvent were used as controls. The pipette was connected to a stimulus air delivery system, and a 0.5-s pulse of compound-laden air was delivered to the antenna. After each stimulation, the next compound was tested only after the sensillum activity had returned to the pre-stimulation baseline. Each recording replicate was conducted using a different midge, and each sensillum was recorded only once. The CO_2 stimulus was pulsed through a separate delivery system that delivered controlled pulses using a PSM 8000 microinjector (WPI) into the same humidified airstream, supplied from 1% CO_2 gas cylinders. Responses to all odorants were normalized by subtracting solvent control responses. Stimuli evoking net responses exceeding 50 spikes/s were defined as strong excitatory responses, whereas those yielding absolute responses below 10 spikes/s were classified as no clear response.

RNA-seq of Heads from Female *F. taiwana*. Total RNA was extracted from the heads of female adults using a TRIzol reagent kit (Invitrogen, Waltham, MA, USA) according to the manufacturer's instructions. After extraction, RNA quality was assessed using an Agilent 2100 Bioanalyzer and verified via RNase-free agarose gel electrophoresis. Each sample consisted of 240 dissected adult midges, with three biological replicates. After RNA quality validation, cDNA libraries were constructed and sequenced on the Illumina platform by Novogene (Beijing, China).

Raw reads were quality-filtered by removing adapter sequences, low-quality reads, and reads containing poly-N. Clean reads were mapped to the reference genome of *F. taiwana* (version GCA_963930915.1) using HISAT2 (version 2.0.5). Gene expression was quantified with RSEM and normalized by TPM. Expression levels of odorant receptor (OR), gustatory receptor (GR), and ionotropic receptor (IR) genes were then analyzed using head transcriptome data from female *F. taiwana*.

Ultralow input transcriptomic RNA-seq of the antennae and maxillary palps. Antennae and maxillary palps were dissected from female adult *F. taiwana* on dry ice and instantly transferred to RNase-free PCR tubes prefilled with lysis sample buffer containing RNase inhibitor. Each biological sample was pooled from two female adults, with three independent biological replicates generated in total. cDNA synthesis and amplification were performed using the Single Cell Full Length mRNA-Amplification Kit (Vazyme, Nanjing, Jiangsu, China) according to the manufacturer's instructions. The cDNA concentration was quantified using a Qubit fluorometer. cDNA libraries were constructed with the TruePrep® Flexible DNA Library Prep Kit for Illumina following the manufacturer's protocols. After library quality verification, sequencing was performed on the sequencing platform at Shenzhen Bay Laboratory.

Raw sequencing reads were quality-trimmed using Trim Galore (version 0.6.10). The trimmed RNA-seq reads were then mapped to the reference genome (version GCA_963930915.1) and quantified at the gene level using Salmon (version 1.10.0). The transcript abundance outputs generated by Salmon were aggregated via the R package tximport and normalized to TPM values. Genes with TPM > 10 were classified as highly expressed in the present study (64, 65).

***The Drosophila* "empty" neuron system.** We performed heterologous expression of *FtaiOrs* in the ab3A empty neuron system following the method described by Chahda et al. (2019) (66). Briefly, specific primers were designed based on the CDS sequences of the top 20 highly expressed Or genes in *F. taiwana* (*SI Appendix*, Table S4). Each *FtaiOr* gene was individually amplified using head cDNA of *F. taiwana* as the template, and cloned into the *pUAST-attB* expression vector. The recombinant plasmid *pUAST-FtaiOrX* was microinjected into embryos via a phiC31 integrase-mediated site-specific transgenic system, yielding a total of 20 transgenic lines *UAS-FtaiOrX*. Subsequently, each *UAS-FtaiOrX* line was crossed with the balancer line (*w; Sp/Cyo;Dr/TM3,sb*) and the empty neuron driver line (*w; Or22ab^{Gal4}/ Or22ab^{Gal4}; Dr/TM3*). The resulting homozygous individuals (*Or22ab^{Gal4};UAS-FtaiOrX*) were verified by PCR for sequence identity, and this functional line was ultimately used for subsequent single-sensillum recordings.

After generating the 20 UAS-FtaiOr fly lines, we crossed them individually with the balancer, then with the driver line for establishing the testing line (*Or22ab^{Gal4};UAS-FtaiOrX*). When we performed SSRs on ab3A neuron (housed in ab3 sensilla) expressing each of these 20 OR genes, we found that 14 of them (*FtaiOr5*, *FtaiOr11*, *FtaiOr14*, *FtaiOr16*, *FtaiOr19*, *FtaiOr26*, *FtaiOr36*, *FtaiOr58*, *FtaiOr61*, *FtaiOr62*, *FtaiOr70*, *FtaiOr75*, *FtaiOr76*, and *FtaiOr79*) failed to be properly expressed in the ab3A neuron with either no large spike (A neuron) or abnormal burst spikes (SI Appendix, Fig. S5). Only ab3A neuron expressing *FtaiOr1*, *FtaiOr12*, *FtaiOr20*, *FtaiOr27*, *FtaiOr60*, and *FtaiOr124* exhibited stable, consistent spikes. A total of 180 volatile compounds (*SI Appendix*, Table S3), including human volatiles compounds, plant volatiles, the common insect repellent DEET, and other ecologically relevant odorants, were used for single-sensillum recording. Compounds were diluted to 1% (v/v for liquid or m/v for solid) using paraffin oil or DMSO. For compounds eliciting strong responses, serial dilutions were prepared at concentrations of 1%, 0.1%, 0.01%, 0.001%, and 0.0001% (v/v).

Whole-mount RNA in situ hybridization. A modified RNASweAMI ISH protocol (GF002, Servicebio) was employed to detect target RNA in whole-mount female antennae. RNA probes targeting the *ORs* (*FtaiOrco, FtaiOr1, FtaiOr27, FtaiOr60*) incorporating the fluorescent dye Cy3 at the 5' ends were designed (*SI Appendix*, Table S5). Briefly, female adult head were dissected and enzymatically digested in a chitinase–chymotrypsin solution [119 mM NaCl, 48 mM KCl, 2 mM $CaCl_2$, 2 mM $MgCl_2$, 25 mM HEPES, 5 U/mL chitinase (Sigma-Aldrich, C6137-50UN), 100 U/mL α-chymotrypsin (Sigma-Aldrich, CHY5S-10VL), 2% DMSO] with gentle rotation at 37 °C for 1 h. Subsequently, the samples were washed three times in PBST (1× PBS containing 0.1% Tween-20) for 10 min each at room temperature. The samples were

then fixed overnight at 4 °C in a solution of 4% paraformaldehyde, 1× PBS, and 0.03% Triton X-100, followed by four 10-min washes in PBST at room temperature. The samples were serially dehydrated in graded methanol/PBST solutions (25%, 50%, 75%, and twice 100%) for 10 min per step at 4 °C, then stored overnight in 100% methanol at −20 °C. On the following day, tissues were serially rehydrated in graded methanol/PBST solutions (75%, 50%, 25%) for 10 min each at 4 °C, then washed twice in PBST for 10 min each at room temperature. The samples were fixed in 4% paraformaldehyde in PBST for 20 min at room temperature and washed three times for 10 min each in PBST at room temperature.

Pre-hybridization was performed at 40°C for 30 min, followed by overnight hybridization with target probe hybridization solution at 40 °C. Post-hybridization washes were performed sequentially in 2×, 1×, 0.5×, and 0.1× saline sodium citrate (SSC) at 40 °C for 30 min each. The samples were then incubated in hybridization solution containing branched DNA probes at 40 °C for 45 min, and washed again under the same conditions. Cy3-labeled signal probes were added at a 1:200 dilution and incubated at 37 °C for 3 h, after which the samples were washed sequentially with 4×,2×, 1×, and 0.5× SSC at 37 °C for 30 min each. The samples were stained with DAPI working solution in the dark at room temperature for 1 h, washed, and mounted in antifade mounting medium. Hybridized samples were imaged using a Zeiss LSM 980 laser scanning confocal microscope equipped with a 63× objective lens (Carl Zeiss Microscopy GmbH, Jena, Germany).

Spatial repellency assay. A modified spatial repellency assay was employed to evaluate the avoidance behavior of *F. taiwana* in response to terpenoids with high electrophysiological activity (67). The experimental apparatus was constructed from acrylic (Figure 4) and consisted of two outer treatment cylinders (15 × 10 cm) and two inner compound-carrying cylinders (13 × 9 cm) arranged in a nested design, along with auxiliary structures including a midge release chamber and connecting segments. Prior to the experiment, trimmed nylon stockings were fitted over the openings of the inner compound-carrying cylinders. Test compound solutions were applied onto the surface of the nylon stockings, after which the inner cylinders were inserted into the outer treatment cylinders to assemble the treatment arms. Nylon stockings treated with blank solvent alone served as the control group. Female midges were placed in the central experimental chamber and allowed to acclimate for 5 minutes. The chamber doors were then opened simultaneously to release the midges, and their responses to the stimuli were recorded for 10 minutes. Subsequently, the number of midges in each chamber was counted, and after each trial, the experimental setup was thoroughly cleaned with 70% ethanol. 20 midges of each strain were used for each experiment, and each treatment was subjected to at least 6 replicates. The repellency index (RI) was calculated as RI = (Nc - Nt) / (Nc + Nt), where Nc and Nt represent the number of midges in the control and treatment chambers, respectively. DEET was used as a positive control.

Y-tube olfactometer assay. The attractive responses of midges to human volatiles with high electrophysiological activity were evaluated using a Y-tube olfactometer. First, the apparatus was assembled in the following order: an oil-free positive-negative pressure vacuum pump;

two drying towers filled with activated carbon; two gas splitters; two flowmeters; two gas-washing bottles; and a behavioral assay device. Before each trial, a filter paper treated with a single test compound was placed in one odor source chamber, while a filter paper treated with solvent alone was placed in the opposite chamber as a control. Female midges were introduced into the insect release arena. After 10 minutes, the number of midges in the compound-containing tube (O) and the control tube (C) was recorded. The experimental apparatus was thoroughly cleaned with 75% ethanol after each trial. 10 midges of each strain were used for each experiment, and each treatment was subjected to at least 6 replicates. The attractiveness of each compound to midges was quantified using the preference index (PI), calculated as PI = (O - C) / T, where T represents the total number of midges used in the assay. The PI ranged from -1 (complete avoidance) to 1 (complete attraction).

Acknowledgments

We thank all members of the Feng Liu Lab at Shenzhen Bay Laborator (SZBL) and Xiaohui Hou lab at Zunyi Medical University for suggestions and comments and the sequencing platform at SZBL for equipment and technical support. We also thank Prof. John Carlson at Yale University for generously providing the balancer fly line and the driver line. This work was supported by the National Natural Science Foundation of China (Grant No. 82502760) to Y.S.; National Natural Science Foundation of China (Grant No. 82372289 and 82561128263), Gates Fundations, and Guangdong Pearl River Funding (Grant No. 2023QN10Y093) awarded to F.L.; Shenzhen Medical Academy of Research and Translation (SMART) (Grant No. A032400171) to S.T.F..

References

1. F. Sick, M. Beer, H. Kampen, K. Wernike, *Culicoides* Biting Midges—Underestimated Vectors for Arboviruses of Public Health and Veterinary Importance. *Viruses* 11, 376 (2019).
2. H. Kampen, D. Werner, Biting midges (Diptera: Ceratopogonidae) as vectors of viruses. *Microorganisms* 11, 2706 (2023).
3. F. G. Naveca et al., Human outbreaks of a novel reassortant Oropouche virus in the Brazilian Amazon region. *Nat. Med.* 30, 3509-3521 (2024).
4. H. M. Moreira et al., Outbreak of Oropouche virus in frontier regions in western Amazon. *Microbiol. Spectr.* 12, e01629 (2024).
5. C. Alkan, T. Ikegami, Emerging threat of Oropouche virus: clinical features, experimental models, and virulence. *Virulence* 17, 2664956 (2026).
6. L. Subissi et al., Oropouche virus: transmission, epidemiology, genetic diversity, and public health implications. *eClinicalMedicine* 95, 103871 (2026).
7. A. Touati, T. Idres, C. De Champs, N. S. Basher, Emerging arthropod-borne infections in temperate regions: comparative synthesis across mosquitoes, ticks, sandflies, and biting midges. *Insects* 17, 311 (2026).

8. L. Harrup, M. A. Miranda, S. Carpenter, Advances in control techniques for *Culicoides* and future prospects. *Vet. Ital.* 52, 247-264 (2016).
9. S. Carpenter, P. S. Mellor, S. J. Torr, Control techniques for *Culicoides* biting midges and their application in the U.K. and northwestern Palaearctic. *Med. Vet. Entomol.* 22, 175-187 (2008).
10. J. B. Pitzer et al., Assessing permethrin susceptibility of field-collected biting midges in Florida and evidence for resistance evolution using laboratory selections. *Med. Vet. Entomol.* (2026).
11. G. Gibson, S. J. Torr, Visual and olfactory responses of haematophagous Diptera to host stimuli. *Med. Vet. Entomol.* 13, 2-23 (1999).
12. F. Guidobaldi, I. J. May-Concha, P. G. Guerenstein, Morphology and physiology of the olfactory system of blood-feeding insects. *J. Physiol. Paris* 108, 96-111 (2014).
13. T. Lu, Y. Zhang, D. Gou, H. Chen, X. Hou, The effects of human volatiles produced by skin microbiota on *Forcipomyia* (*Lasiohelea*) *taiwana* host preference. *Pest Manag. Sci.* 81, 7815-7826 (2025).
14. C. Montell, The sensory arsenal mosquitoes use to find us. *Trends Parasitol.* 41, 591-602 (2025).
15. J. Fleischer, P. Pregitzer, H. Breer, J. Krieger, Access to the odor world: olfactory receptors and their role for signal transduction in insects. *Cell. Mol. Life Sci.* 75, 485-508 (2018).
16. C. J. McMeniman, R. A. Corfas, B. J. Matthews, S. A. Ritchie, L. B. Vosshall, Multimodal integration of carbon dioxide and other sensory cues drives mosquito attraction to humans. *Cell* 156, 1060-1071 (2014).
17. M. Herre et al., Non-canonical odor coding in the mosquito. *Cell* 185, 3104-3123.e3128 (2022).
18. M. C. Stensmyr et al., A conserved dedicated olfactory circuit for detecting harmful microbes in *Drosophila*. *Cell* 151, 1345-1357 (2012).
19. A. F. Carey, G. Wang, C. Y. Su, L. J. Zwiebel, J. R. Carlson, Odorant reception in the malaria mosquito *Anopheles gambiae*. *Nature* 464, 66-71 (2010).
20. E. A. Hallem, J. R. Carlson, Coding of odors by a receptor repertoire. *Cell* 125, 143-160 (2006).
21. E. Isberg, Y. Hillbur, R. Ignell, Comparative study of antennal and maxillary palp olfactory sensilla of female biting midges (Diptera: Ceratopogonidae: *Culicoides*) in the context of host preference and phylogeny. *J. Med. Entomol.* 50, 485-492 (2013).
22. G. Sollai, P. Solari, C. Masala, R. Crnjar, A. Liscia, Effects of avermectins on olfactory responses of *Culicoides imicola* (Diptera: Ceratopogonidae). *J. Med. Entomol.* 44, 656-659 (2007).
23. A. Bhasin, A. J. Mordue, W. Mordue, Electrophysiological and behavioural identification of host kairomones as olfactory cues for *Culicoides impunctatus* and *C. nubeculosus*. *Physiol. Entomol.* 25, 6-16 (2000).
24. M. D. Lin et al., Decoding the genome of bloodsucking midge *Forcipomyia taiwana* (Diptera:

Ceratopogonidae): insights into odorant receptor expansion. *Insect Biochem. Mol. Biol.* 168, 104115 (2024).

25. A. Borkent, P. Dominiak, Catalog of the biting midges of the world (Diptera: Ceratopogonidae). *Zootaxa* 4787, 1-377 (2020).
26. Y. Yu, Important hematophagous midges of China. Science Press, Beijing (2019).
27. Y. Chen et al., Hypersensitivity to *Forcipomyia taiwana* (biting midge): clinical analysis and identification of major For t 1, For t 2 and For t 3 allergens. *Allergy* 60, 1518-1523 (2005).
28. H. Shu, C. Chen, Y. Hsu, G. Lin, A pilot study for the establishment of a bloodsucking model for *Forcipomyia taiwana* (biting midge). *Int. J. Clin. Med. Microbiol.* 2, 118 (2017).
29. C. Chen, J. Lien, Y. Lin, S. Hsu, The diurnal biting pattern of a bloodsucking midge *Forcipomyia* (*Lasiohelea*) *taiwana* (Shiraki) (Diptera: Ceratopogonidae). *Chin. J. Microbiol. Immunol.* 14, 54-56 (1981).
30. Y. H. Chen, G. Y. Hwang, P. C. Chen, W. C. Tu, M. F. Lee, Molecular cloning and immunologic characterization of For t 2: a major allergen from the biting midge *Forcipomyia taiwana*. *Allergy* 66, 703-705 (2011).
31. X. L. Guo, Z. H. Yang, Research progress on vectors of Japanese encephalitis in China. *Chin. J. Vector Biol. Control* 30, 106-110 (2019).
32. J. R. Wu, S. Y. Wu, Isolation of Japanese encephalitis virus from *Lasiohelea taiwana* (Ceratopogonidae). *Acta Microbiol. Sin.* 5, 22-26 (1957).
33. U. R. Bernier, D. L. Kline, D. R. Barnard, C. E. Schreck, R. A. Yost, Analysis of human skin emanations by gas chromatography/mass spectrometry. 2. Identification of volatile compounds that are candidate attractants for the yellow fever mosquito *Aedes aegypti*. *Anal. Chem.* 72, 747-756 (2000).
34. J. M. Kembro, R. H. Marin, J. A. Zygadlo, R. M. Gleiser, Effects of the essential oils of *Lippia turbinata* and *Lippia polystachya* (Verbenaceae) on the temporal pattern of locomotion of the mosquito *Culex quinquefasciatus* (Diptera: Culicidae) larvae. *Parasitol. Res.* 104, 1119-1127 (2009).
35. Y. Vainer et al., Sensory coding of borneol repellency in culicine mosquitoes via the Or49 pathway. *Nat. Commun.* 17, 2981 (2026).
36. F. Liu, Z. Ye, A. Baker, H. Sun, L. J. Zwiebel, Gene editing reveals obligate and modulatory components of the CO_2 receptor complex in the malaria vector mosquito, *Anopheles coluzzii*. *Insect Biochem. Mol. Biol.* 127, 103470 (2020).
37. P. L. Jones, G. M. Pask, D. C. Rinker, L. J. Zwiebel, Functional agonism of insect odorant receptor ion channels. *Proc. Natl. Acad. Sci. U.S.A.* 108, 8821-8825 (2011).
38. D. K. Yadav, S. Rathee, V. Sharma, U. K. Patil, A comprehensive review on insect repellent agents: medicinal plants and synthetic compounds. *Anti-Inflamm. Anti-Allergy Agents Med. Chem.* 24, 84-102 (2025).
39. P. C. Page, K. Labuschagne, J. P. Nurton, G. J. Venter, A. J. Guthrie, Duration of repellency of N,N-diethyl-3-methylbenzamide, citronella oil and cypermethrin against *Culicoides* species when applied to polyester mesh. *Vet. Parasitol.* 163, 105-109 (2009).

40. C. R. Lazzari, Why do repellents repel? *Curr. Opin. Insect Sci.* 66, 101277 (2024).
41. N. K. T. Thomas, C. Berry, I. S. Sobhy, Making scents of mosquito lures: semiochemical attractants for adult mosquitoes. *Parasites Vectors* (2026).
42. W. Liu, S. Lee, E. Yang, Evaluation for attractiveness of four chemicals to the biting midge, *Forcipomyia taiwana* (Diptera: Ceratopogonidae). *J. Am. Mosq.* Control Assoc. 25, 448-455 (2009).
43. J. G. Logan et al., Identification of human-derived volatile chemicals that interfere with attraction of *Aedes aegypti* mosquitoes. *J. Chem. Ecol.* 34, 308-322 (2008).
44. Y. T. Qiu, J. J. A. van Loon, W. Takken, J. Meijerink, H. M. Smid, Olfactory coding in antennal neurons of the malaria mosquito, *Anopheles gambiae*. *Chem. Senses* 31, 845-863 (2006).
45. M. Ghaninia, R. Ignell, B. S. Hansson, Functional classification and central nervous projections of olfactory receptor neurons housed in antennal trichoid sensilla of female yellow fever mosquitoes, *Aedes aegypti*. *Eur. J. Neurosci.* 26, 1611-1623 (2007).
46. N. M. Stanczyk, J. F. Y. Brookfield, R. Ignell, J. G. Logan, L. M. Field, Behavioral insensitivity to DEET in *Aedes aegypti* is a genetically determined trait residing in changes in sensillum function. *Proc. Natl. Acad. Sci. U.S.A.* 107, 8575-8580 (2010).
47. R. Benton, K. S. Vannice, C. Gomez-Diaz, L. B. Vosshall, Variant ionotropic glutamate receptors as chemosensory receptors in *Drosophila*. *Cell* 136, 149-162 (2009).
48. Z. Ye, F. Liu, H. Sun, A. P. Baker, L. J. Zwiebel, Discrete roles of Ir76b ionotropic coreceptor impact olfaction, blood feeding, and mating in the malaria vector mosquito *Anopheles coluzzii*. *Proc. Natl. Acad. Sci. U.S.A.* 119, e2112385119 (2022).
49. T. Lu et al., Odor coding in the maxillary palp of the malaria vector mosquito *Anopheles gambiae*. *Curr. Biol.* 17, 1533-1544 (2007).
50. G. Wang, A. F. Carey, J. R. Carlson, L. J. Zwiebel, Molecular basis of odor coding in the malaria vector mosquito *Anopheles gambiae*. *Proc. Natl. Acad. Sci. U.S.A.* 107, 4418-4423 (2010).
51. X. Wang et al., Heterologous expression and functional analysis of *Aedes aegypti* odorant receptors to human odors in *Xenopus oocytes*. *J. Vis. Exp.* 172, e61813 (2021).
52. F. Miazzi et al., Optimization of insect odorant receptor trafficking and functional expression via transient transfection in HEK293 cells. *Chem. Senses* 44, 673-682 (2019).
53. J. H. Pettersson, A. M. Cattaneo, Heterologous investigation of metabotropic and ionotropic odorant receptors in ab3A neurons of *Drosophila melanogaster*. *Front. Mol. Biosci.* 10, 1275901 (2024).
54. A. Ysobel et al., A review on the potential and efficacy of plant-based mosquito repellents against DEET-based mosquito repellents. *In SHS Research Conference Proceedings* (De La Salle University, Manila) (2022).
55. W. Wu et al., Study of the repellent activity of 60 essential oils and their main constituents against *Aedes albopictus*, and nano-formulation development. *Insects* 13, 1077 (2022).
56. J. G. Logan, M. A. Birkett, Semiochemicals for biting fly control: their identification and

exploitation. *Pest Manag. Sci.* 63, 647-657 (2007).

57. L. Dormont, M. Mulatier, D. Carrasco, A. Cohuet, Mosquito attractants. *J. Chem. Ecol.* 47, 351-393 (2021).

58. R. Yan et al., Molecular and functional characterization of a conserved odorant receptor from *Aedes albopictus*. *Parasites Vectors* 15, 43 (2022).

59. M. A. de Souza et al., Adulticide and repellent activity of essential oils against *Aedes aegypti* (Diptera: Culicidae) – a review. *S. Afr. J. Bot.* 124, 160-165 (2019).

60. H. Zhang et al., A volatile from the skin microbiota of flavivirus-infected hosts promotes mosquito attractiveness. *Cell* 185, 2510-2522.e16 (2022).

61. E. J. Huang, J. Q. Zhang, Y. S. Cai, Y. H. Zhong, B. Gao, Application of CO Ⅰ and 16S rDNA genes in the identification of *Lasiohelea taiwana*. *China Port Sci. Technol.* 2, 4-8 (2021).

62. J. Pelletier, A. Guidolin, Z. Syed, A. J. Cornel, W. S. Leal, Knockdown of a mosquito odorant-binding protein involved in the sensitive detection of oviposition attractants. *J. Chem. Ecol.* 36, 245-248 (2010).

63. F. Liu et al., A dual-target molecular mechanism of pyrethrum repellency against mosquitoes. *Nat. Commun.* 12, 2553 (2021).

64. Z. Li, M. Li, J. Wang, Asymmetric subgenomic chromatin architecture impacts on gene expression in resynthesized and natural allopolyploid *Brassica napus*. *Commun. Biol.* 5, 762 (2022).

65. A. Poulet, A. J. Kratkiewicz, D. Li, J. C. van Wolfswinkel, Chromatin analysis of adult pluripotent stem cells reveals a unique stemness maintenance strategy. *Sci. Adv.* 9, eadh4887 (2023).

66. J. S. Chahda et al., The molecular and cellular basis of olfactory response to tsetse fly attractants. *PLoS Genet.* 15, e1008005 (2019).

67. X. Wang et al., DEET olfactory reception in the yellow fever mosquito. Preprint, *LangTaoSha Preprint Server* (2026).

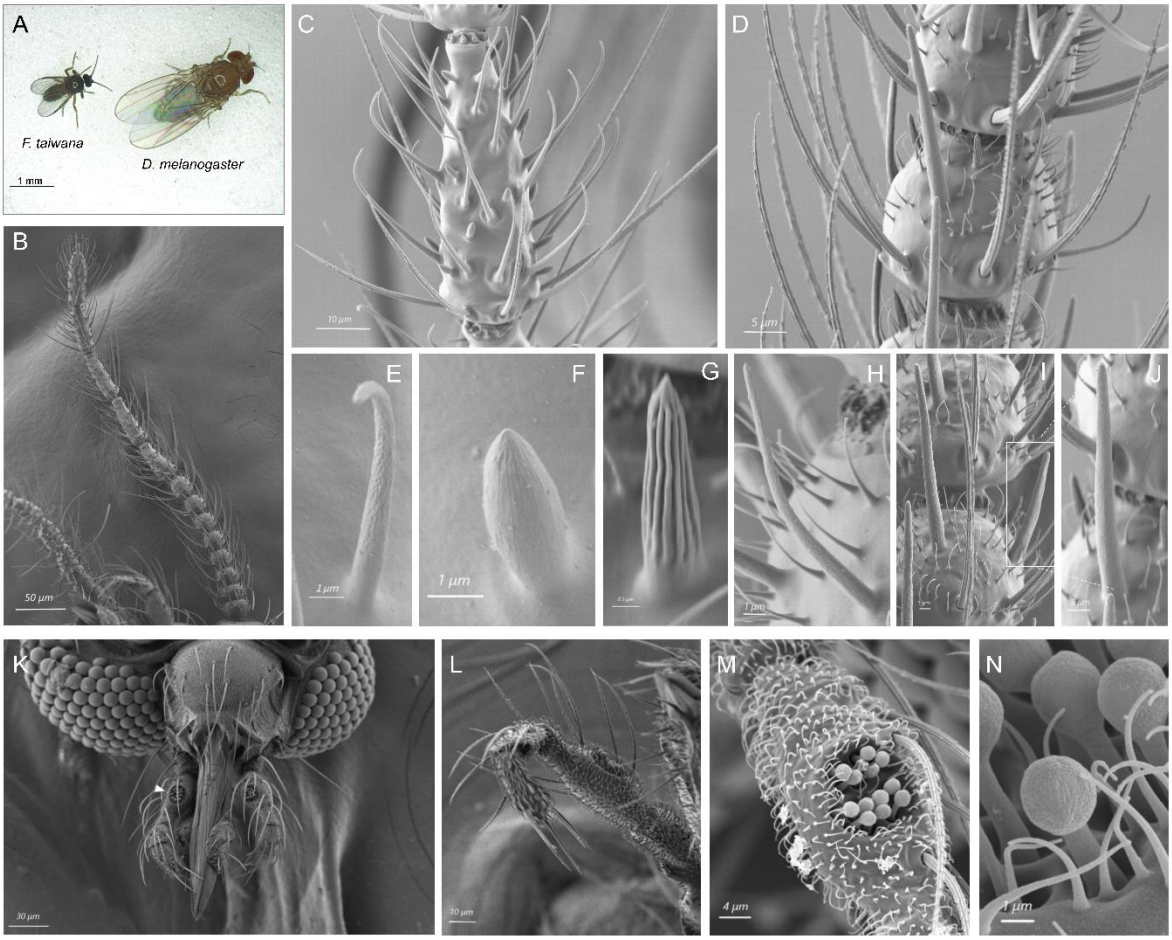

Fig. 1. Scanning electron micrographs of the antenna and maxillary palp of *F. taiwana*. (*A*) Photograph of *D. melanogaster* and *F. taiwana*. (*B*) The morphology of antennal flagellomeres in *F. taiwana.* (*C*) A representative image of an elongated flagellum characteristic of the distal portion of the antenna. (*D*) A representative image of a short flagellum characteristic of the proximal antenna. Representative images of sensillar macrostructure, including (*E*) long sharp trichoid sensilla (LST), (*F*) grooved peg sensilla I (GP I), (*G*) grooved peg sensilla II (GP II), (H) short sharp trichoid sensilla (SST), (*I*) long blunt trichoid sensilla (LBT), and (*J*) short blunt trichoid sensilla (SBT). (*K*) Morphology of the maxillary palp in *F. taiwana*. Representative images of sensillar macrostructure, including (*L*-*M*) a sensillary pit on the third segment of maxillary palp and (*N*) spherical sensilla within the sensillary pit. Scale bars: 1 mm (*A*), 50 μm (*B*), 10 μm (*C*,*L*), 5 μm (*D*), 1 μm (*E*,*F*,*H*,*I*,*N*), 0.5 μm (*G*), 2 μm (*J*), 30 μm (*K*), 4 μm (*M*).

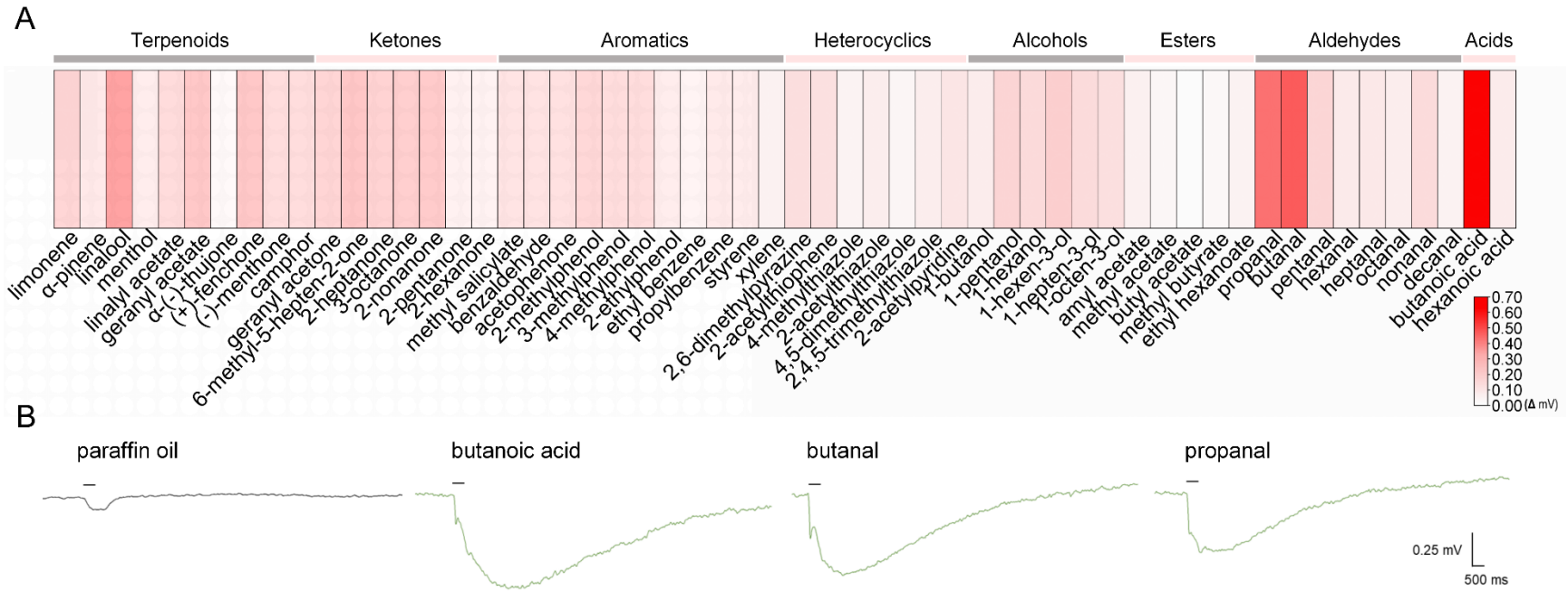

858

859 **Fig. 2.** EAG responses of *F. taiwana* to 56 compounds. (*A*) Heatmap of EAG responses of female adult *F. taiwana* to 56 plant and host-derived
860 volatiles spanning multiple chemical categories, including terpenoids, ketones, aromatics, heterocyclics, alcohols, esters, aldehydes and
861 carboxylic acids. Response intensities are color-coded according to the continuous color scale at the bottom right (unit: Δ mV). All
862 electroantennogram signals elicited by each odorant at a dilution of 10^{-1} were normalized to the solvent control (paraffin oil). (*B*) Representative
863 EAG response traces of female adult *F. taiwana* to butanoic acid, butanal, and propanal.

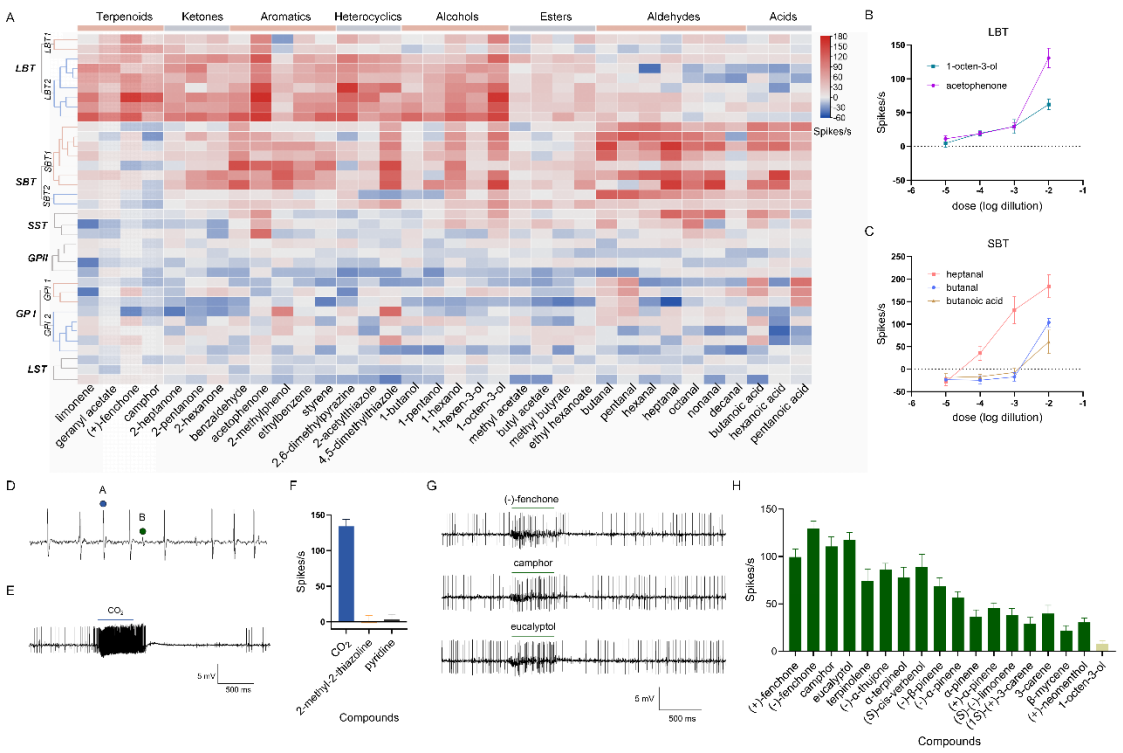

Fig. 3. Single sensillum recording of the antennae and maxillary palps of *F. taiwana.* (*A*) Heatmap showing electrophysiological responses of six olfactory sensilla types (LBT, SBT, SST, GPII, GPI, LST) on antennal flagellum to 34 odor compounds. Compounds are grouped by chemical classes at the top. Response intensities are color-coded according to the continuous color scale on the right (unit: Spikes/s). (*B*) Dose-response curves of LBT sensilla to 1-octen-3-ol and acetophenone. (*C*) Dose-response curves of SBT sensilla to heptanal, butanal and butanoic acid. (*D*) SSR from spherical sensilla located in the sensory pits on the maxillary palps of *F. taiwana*. This sensillum houses two olfactory receptor neurons (A and B), which can be discerned by spike amplitude. (*E*) Representative SSR traces indicating increased firing of A neurons within spherical sensilla upon CO_2 stimulation in female midges. (*F*) The A neurons exhibited robust responses to carbon dioxide (CO_2), while showing no activity to 2-methyl-2-thiazoline and pyridine. (*G*) Representative SSR traces illustrate enhanced spike firing of B neurons in spherical sensilla stimulated with (-)-fenchone, camphor, and eucalyptol. (*H*) Odorant response profiles of the B neurons in spherical sensillum.

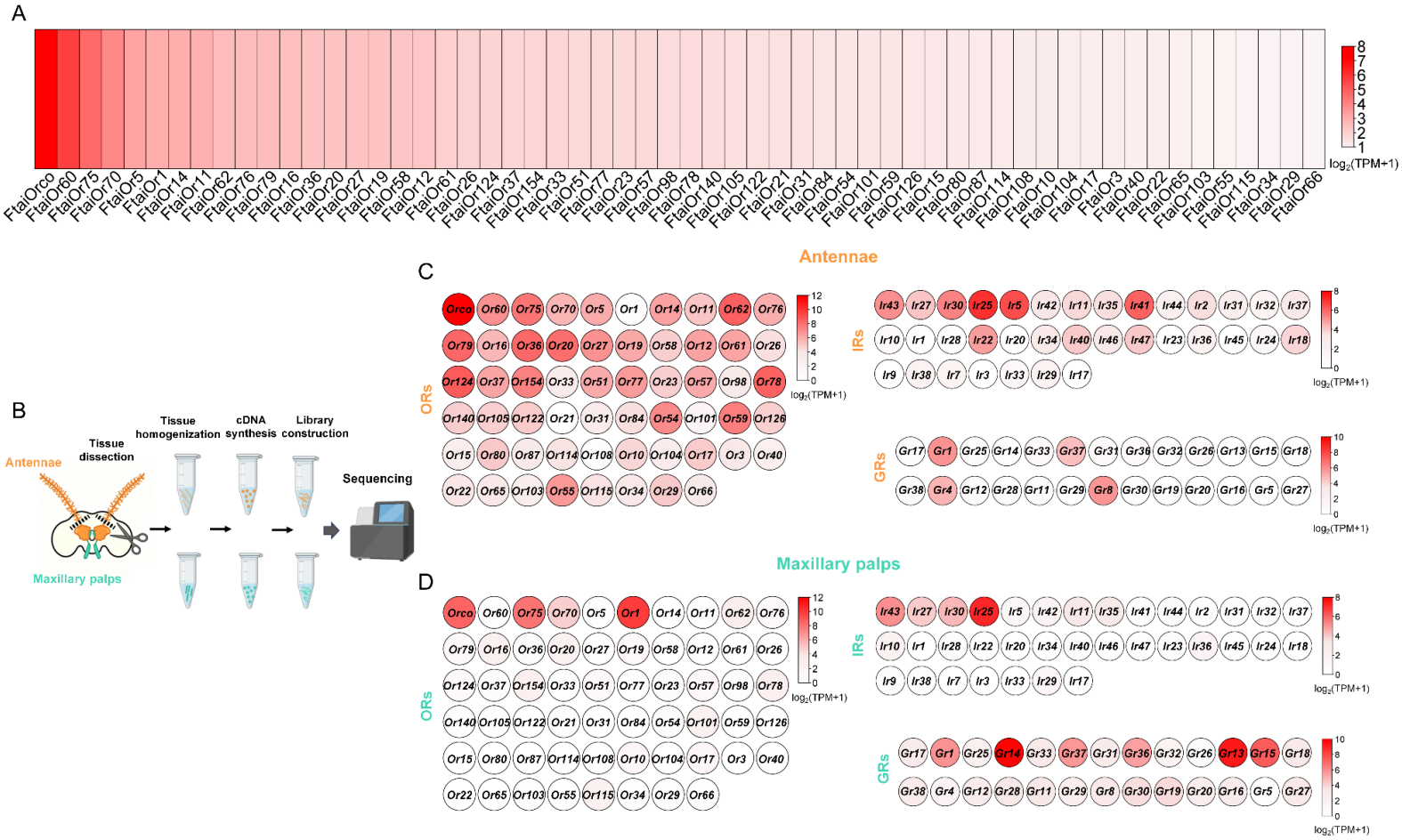

Fig. 4. Expression profiling of chemosensory receptor genes. (*A*) The 58 ORs with substantial expression in the head of female *F. taiwana* adults (TPM>1). Expression levels are presented as $\log_2$(TPM+1). (*B*) SMART-seq of antennae and maxillary palps. (*C, D*) Expression profiles of 58 ORs, 35 IRs, and 26 GRs that are substantially expressed in the head of female *F. taiwana* adults, between antennae and maxillary palps.

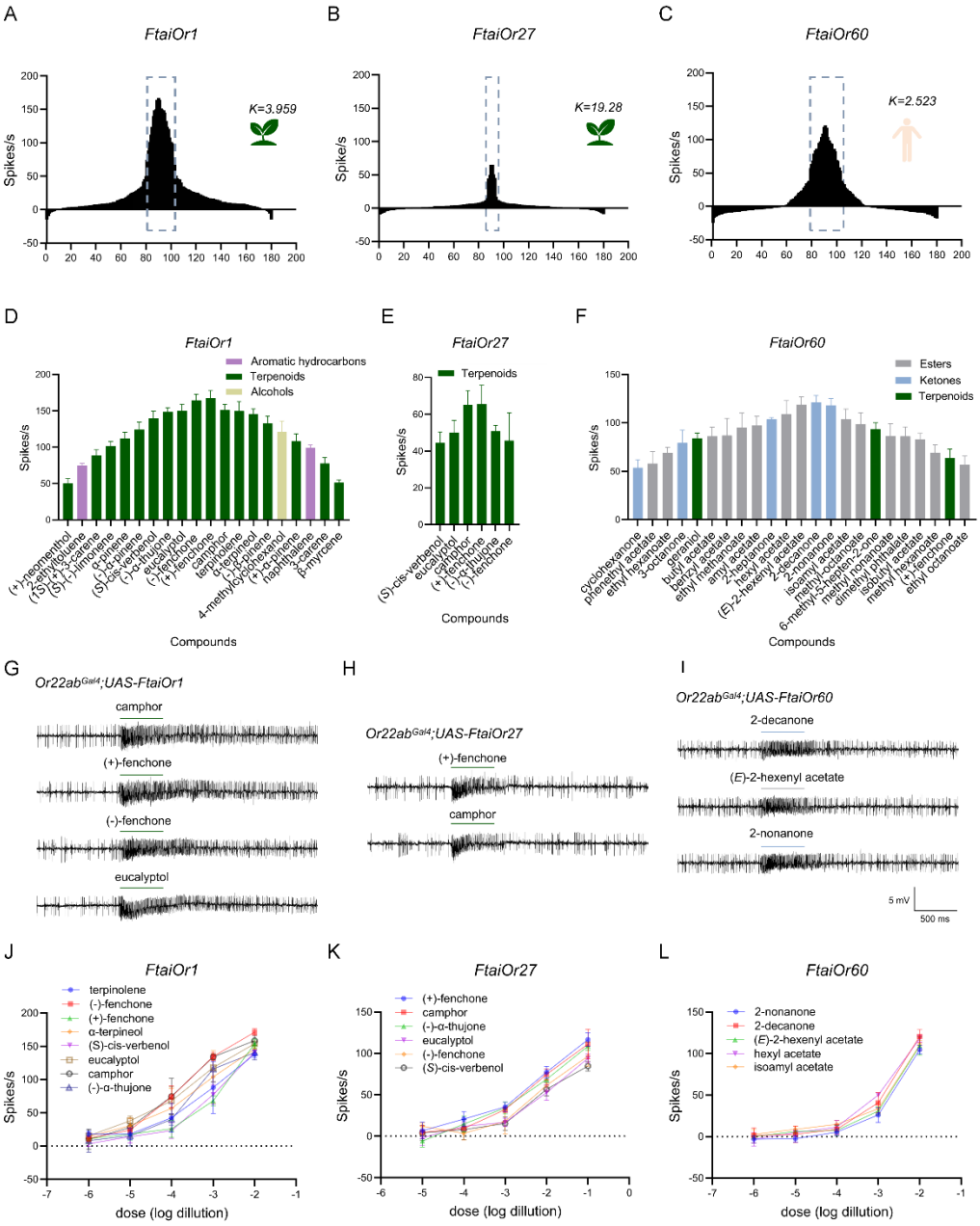

Fig. 5. Functional characterization of the FtaiOrs. (*A*, *B*, *C*) Tuning curves of *FtaiOr1*, *FtaiOr27* and *FtaiOr60* to 180 odorants. The responses of the three FtaiOrs receptors are sorted along the X-axis according to their response magnitudes to each odorant. The receptor with the strongest response is located at the center of the distribution, while those with the weakest responses lie at the edges. Accordingly, the arrangement order of receptors differs for each odorant. The kurtosis value is indicated in each plot. (*D*) Twenty compounds that significantly activate *FtaiOr1* (> 50 spikes/s). (*E*) Six compounds with effective activation of *FtaiOr27* (> 30 spikes/s). (*F*) Twenty-three compounds that significantly activate *FtaiOr60* (> 50 spikes/s). (*G*, *H*, *I*) Representative SSR traces from *Drosophila* ab3A empty neurons expressing *FtaiOr1, FtaiOr27 and FtaiOr60* to compounds. (*J*, *K*, *L*) Dose-response curves for FtaiOr1, FtaiOr27 and FtaiOr60 against potent compounds.

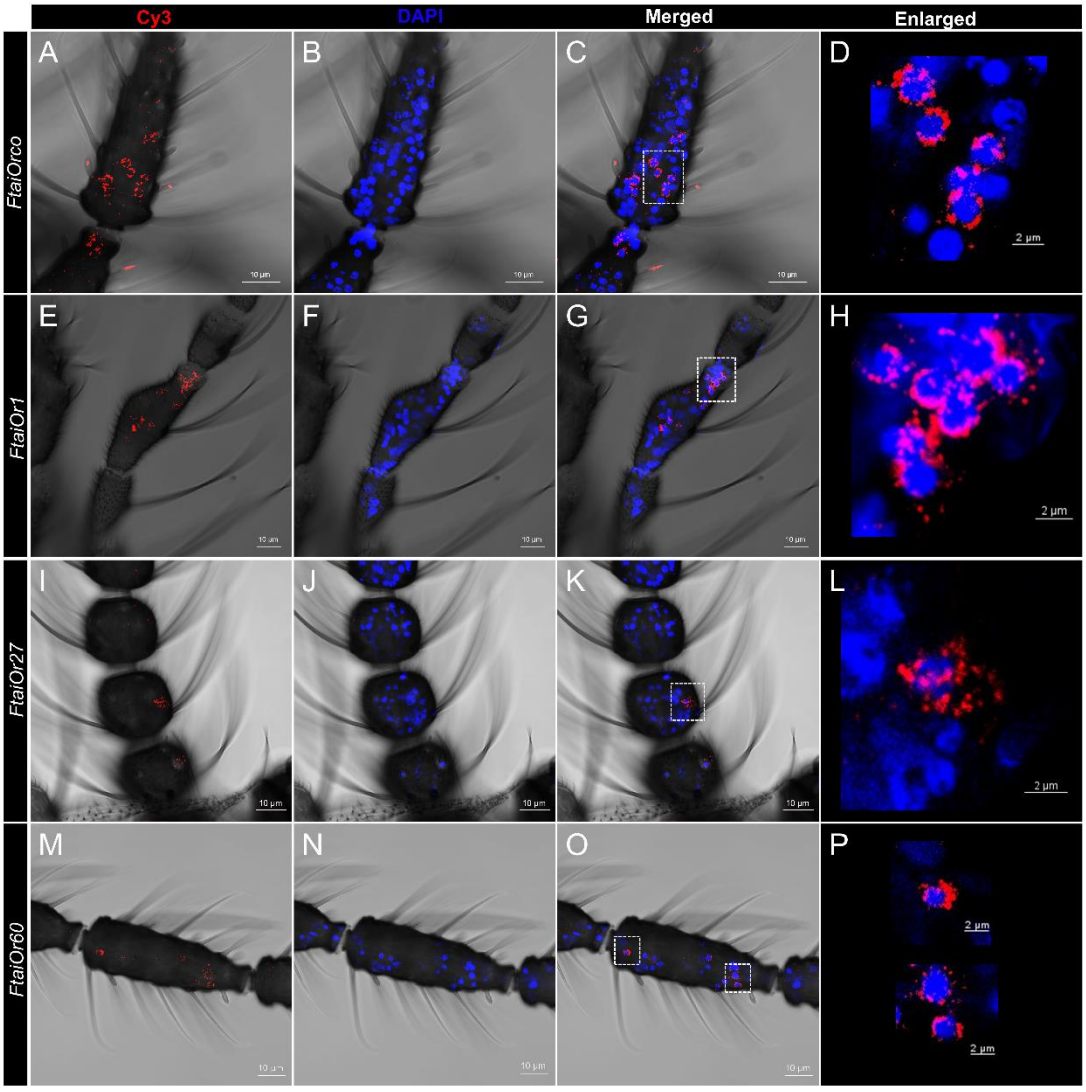

Fig. 6. Localization of *FtaiOrco*, *FtaiOr1*, *FtaiOr27* and *FtaiOr60* transcripts in the antennae and maxillary palps of female *F. taiwana* via whole-mount fluorescence in situ hybridization (WM-FISH). (*A-D*) WM-FISH detection of *FtaiOrco* in antennae. (*E-H*) WM-FISH detection of *FtaiOr1* in maxillary palps. (*I-L*) WM-FISH detection of *FtaiOr27* in antennae. (*M-P*) WM-FISH detection of *FtaiOr60* in antennae. Fluorescent signals of target transcripts labeled by antisense probes are shown in red; nuclei were counterstained with DAPI (blue).

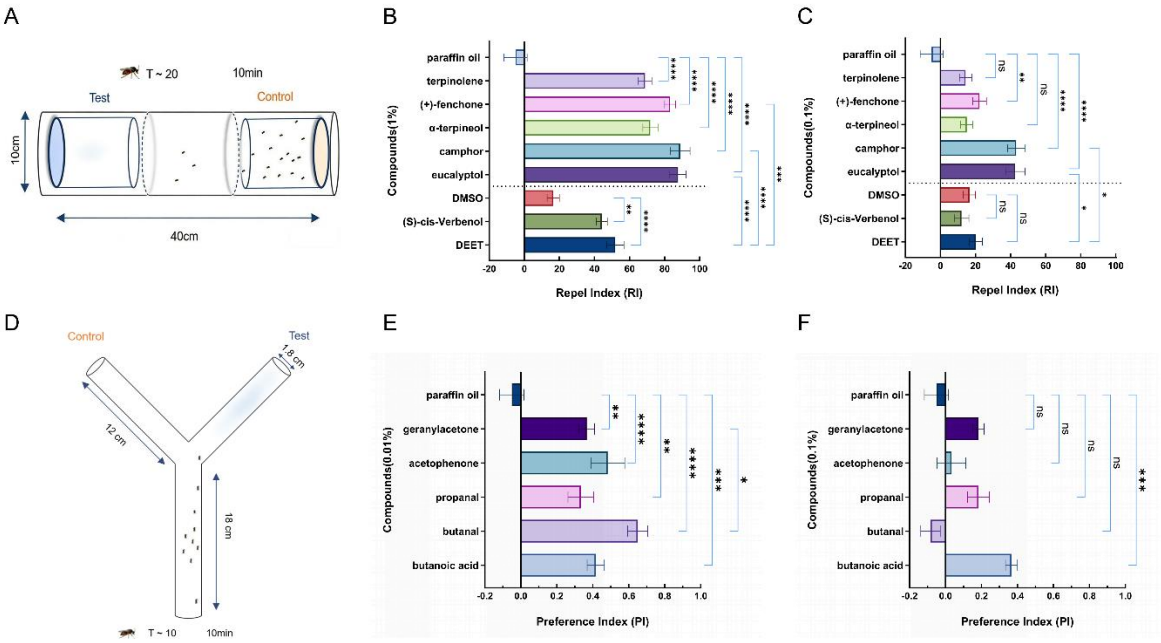

Fig. 7. Behavioral responses of female *F. taiwana* adults to different compounds. (*A*) Schematic drawing of the standard WHO spatial repellency assay. (*B*,*C*) Repellency indices of six terpenoids and DEET against female adult *F. taiwana* at concentrations of 1% and 0.1%. Schematic diagram of Y-tube olfactometer. (*D*) Schematic diagram of Y-tube olfactometer. (*E*,*F*) Preference indices of female adult *F. taiwana* for five human volatiles at concentration of 0.01% and 0.1%. Means were compared using one-way ANOVA, followed by Tukey's test for pairwise comparison against solvent control (paraffin oil, DMSO) or positive control (DEET, geranylacetone) for all odorants. n = 6 replicates for all odorants. Statistical significance was presented as $P < 0.05$ (*), $P < 0.01$ (**), $P < 0.001$ (***), $P < 0.0001$ (****).